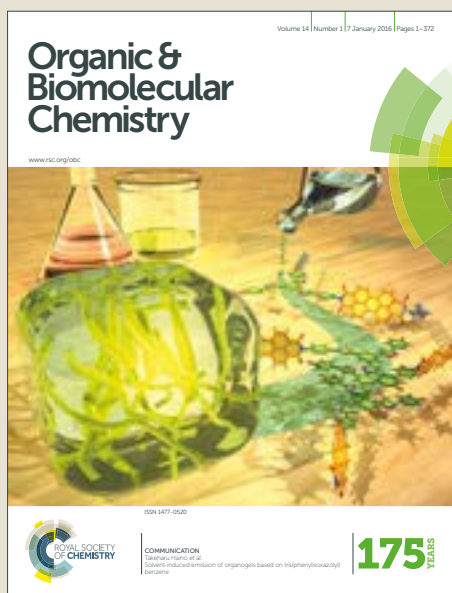


Organic & Biomolecular Chemistry

Accepted Manuscript



This article can be cited before page numbers have been issued, to do this please use: X. Liu, L. Niu, Y. Chen, M. Zheng, Y. yang and Q. Yang, *Org. Biomol. Chem.*, 2016, DOI: 10.1039/C6OB02407F.



This is an Accepted Manuscript, which has been through the Royal Society of Chemistry peer review process and has been accepted for publication.

Accepted Manuscripts are published online shortly after acceptance, before technical editing, formatting and proof reading. Using this free service, authors can make their results available to the community, in citable form, before we publish the edited article. We will replace this Accepted Manuscript with the edited and formatted Advance Article as soon as it is available.

You can find more information about Accepted Manuscripts in the [author guidelines](#).

Please note that technical editing may introduce minor changes to the text and/or graphics, which may alter content. The journal's standard [Terms & Conditions](#) and the ethical guidelines, outlined in our [author and reviewer resource centre](#), still apply. In no event shall the Royal Society of Chemistry be held responsible for any errors or omissions in this Accepted Manuscript or any consequences arising from the use of any information it contains.



Journal Name

COMMUNICATION

A mitochondria-targeting fluorescent probe for the selective detection of glutathione in living cells

Xue-Liang Liu^a, Li-Ya Niu,^{b,*} Yu-Zhe Chen^c, Mei-Ling Zheng^c, Yunxu Yang^{a,*}, and Qing-Zheng Yang^{b,*}

Received 00th January 20xx,
Accepted 00th January 20xx

DOI: 10.1039/x0xx00000x

www.rsc.org/

We report a fluorescent probe for the selective detection of mitochondrial glutathione (GSH). The probe, containing a triphenylphosphine as mitochondrial targeting group, exhibited ratiometric and selective detection of GSH over Cys/Hcy. The probe was used for imaging mitochondrial GSH in living HeLa cells.

Mitochondrion is a double membrane-bound organelle in eukaryotic cells, utilizing oxygen to generate adenosine triphosphate (ATP) as the source of biochemical energy, thus has been described as the powerhouse of the cells¹. In addition, they are involved in many biological processes, such as signaling, cellular differentiation, cell death, and maintaining control of the cell cycle and cell growth². Mitochondria are recognized as a significant source of reactive oxygen species (ROS), which can damage mitochondrial membrane and hinder intracellular oxidative phosphorylation.³ The oxidative damage to the mitochondria is responsible for cell signaling and cell death which cause many neurodegenerative diseases and pathologies, such as Alzheimer's disease, Parkinson's disease, neurodegenerative disorders, etc⁴. As the most abundant biothiols in cells, GSH plays a key role in maintaining the redox environment in mitochondria to avoid or repair oxidative damage⁵. Therefore, it is of great importance to monitor mitochondrial GSH in living cells.

Fluorescence probes are considered to be one of the most efficient molecular tools monitor and visualize analytes in living cells and tissues due to their high sensitivity and selectivity, high spatiotemporal resolution, and real-time imaging⁶. Given that biothiols, including GSH, Cys and Hcy, play

different roles in biological system, the development of fluorescent probes which can distinguish Cys/Hcy/GSH from each other has emerged as an active topic in recent years⁷. However, few probes have been developed to selectively detect mitochondrial GSH⁸. Herein, we reported a fluorescent probe for the selective detection of GSH in mitochondria of the living cells. The probe was composed of chlorinated BODIPY as GSH recognition group and a typical mitochondrial-targeting moiety of triphenylphosphonium cation. It showed a ratiometric fluorescent response towards GSH, while Cys/Hcy induced on-off fluorescence signals. More importantly, it successfully detected mitochondrial GSH in living HeLa cells.

In our previous work^{7b,9}, we developed a BODIPY-based fluorescent probe for the selective detection of GSH over Cys/Hcy. The probe bearing a chlorine at 3-position as a leaving group reacted with thiols by nucleophilic aromatic substitution (S_NAr) to afford thioether. The amino groups of Cys/Hcy but not GSH further went through an intramolecular rearrangement to yield the amino derivatives. The distinct photophysical properties of thioether- and amino- substituted BODIPY enabled the selective detection of GSH. On the other hand, a functional group can be introduced at 5-position through click reaction (e.g., a triethyleneglycol group to improve the water-solubility of the probe). In order to develop a fluorescent probe processing both GSH detection and mitochondrial-targeting ability, a mitochondrial-targeted functional group is necessary. Positively charged groups, especially triphenylphosphonium moiety, are commonly used as mitochondrial delivery vehicles¹⁰. Because the mitochondrial membrane spans across a negative potential, probes with these positive charge take advantage of electrostatic forces to deliver the probe to the mitochondria¹¹. Therefore, our fluorescent probe was designed by integrating triphenylphosphonium moiety into the chlorinated BODIPY.

BODIPY-PPh₃ was synthesized from 3,5-dichlorinated BODIPY as a precursor. First, a trimethylsilylacetylene was attached to the 3-position through Sonogashira coupling. Then the triphenylphosphonium group was introduced by the one pot reaction of the desilylation and click reaction (Scheme 1).

^a School of Chemistry and biological Engineering, University of Science and Technology Beijing, Beijing 100083, P. R. China.

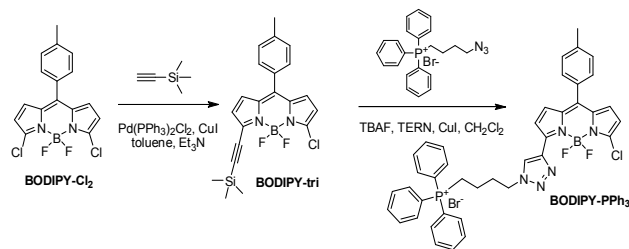
^b Key Laboratory of Radiopharmaceuticals, Ministry of Education, College of Chemistry, Beijing Normal University, Beijing 100875, P. R. China.

^c Key Laboratory of Photochemical Conversion and Optoelectronic Materials, Technical Institute of Physics and Chemistry, Chinese Academy of Sciences, Beijing 100190, P. R. China

Electronic Supplementary Information (ESI) available: [details of any supplementary information available should be included here]. See DOI: 10.1039/x0xx00000x

COMMUNICATION

Compound **BODIPY-PPh₃** was well characterized by ¹H NMR and ¹³C NMR spectroscopy and high-resolution mass spectrometry (HRMS).



Scheme 1 Synthesis of **BODIPY-PPh₃**

At first, we performed the time-dependent absorption and fluorescence response of **BODIPY-PPh₃** in the presence of GSH in HEPES buffer. As shown in Fig. 1, in the presence of GSH, the absorption band of free **BODIPY-PPh₃** centred at 540 nm gradually decreased with concomitant growth of a new band at 570 nm. In the fluorescence spectra, the free **BODIPY-PPh₃** exhibited an emission band at 557 nm. Upon addition of GSH, the original emission at 557 nm decreased, and a new emission band centred at 588 nm increased significantly when excited at the isosbestic point of 550 nm. The ratio of fluorescence intensities at 588 nm and 557 nm (I_{588}/I_{557}) showed good linear relationship with the GSH concentrations (0–80 μ M, $R^2 = 0.993$), and the detection limit was determined to be 1.1 μ M ($S/N = 3$).

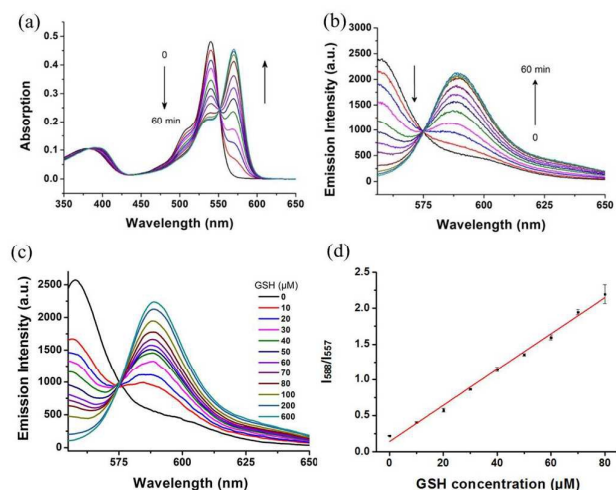


Fig. 1 Time-dependent (a) absorption and (b) emission spectra of **BODIPY-PPh₃** (10 μ M) in the presence of 1 mM GSH. (c) Fluorescence spectra of **BODIPY-PPh₃** (10 μ M) after 1 h upon addition of increasing concentrations of GSH. (d) The fluorescence ratio of 588 nm and 557 nm (I_{588}/I_{557}) as a function of the GSH concentration (0 to 80 μ M). $\lambda_{ex} = 550$ nm. Each spectrum was obtained in acetonitrile/ HEPES buffer (5:95, v/v, 20 mM, pH 7.4) at 37 $^{\circ}$ C.

The spectroscopic responses of **BODIPY-PPh₃** to Cys and Hcy were also investigated (Fig. S1 and S2). Upon addition of Cys, the absorption at 540 nm decreased gradually, and a blue-

shifted absorption band at 500 nm was observed. Meanwhile, the fluorescence at 557 nm turned off gradually. In the case of Hcy, with the decrease of the absorption at 540 nm, an absorption band centred at 570 nm emerged and increased at the initial 40 min. Then the absorption at 570 nm decreased with the appearance of a blue-shifted absorption band at 500 nm. The emission intensity at 557 nm gradually decreased, with the simultaneous enhancement of the fluorescence at 588 nm initially. As the reaction progressed, the fluorescence intensity at 588 nm decreased. The absorption and emission spectra of **BODIPY-PPh₃** in the presence of GSH, Cys and Hcy were shown in Fig. 2, indicating **BODIPY-PPh₃** selectively detected GSH over Cys/Hcy.

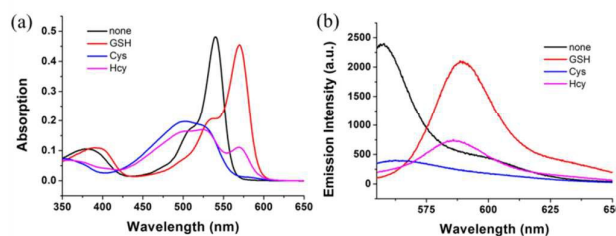
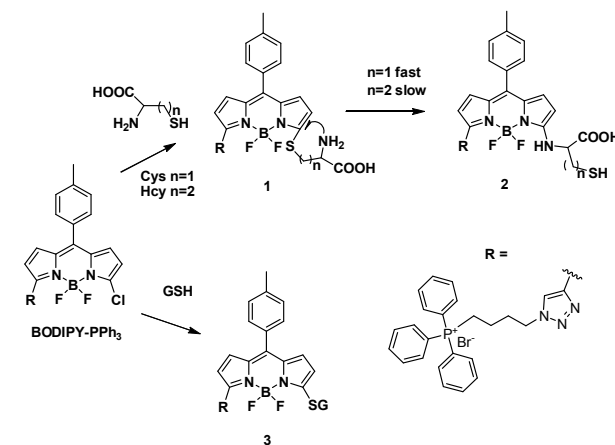


Fig. 2 (a) Absorption and (b) fluorescence spectra of **BODIPY-PPh₃** (10 μ M) upon addition of 1 mM GSH, Cys and Hcy in acetonitrile/ HEPES buffer (5:95, v/v, 20 mM, pH 7.4) after 3 h addition at 37 $^{\circ}$ C. $\lambda_{ex} = 550$ nm.



Scheme 2 Reaction mechanism for **BODIPY-PPh₃** with Cys, GSH and Hcy.

The spectroscopic properties of **BODIPY-PPh₃** were in good agreement with our previous studies. Based on the above observation and previous explorations, we proposed the reaction mechanism, as illustrated in Scheme 2. Initially, the chloro leaving group is replaced by the thiols through the thiol-halogen S_NAr nucleophilic substitution to produce compound **1** and **3**. For Cys/Hcy, once **1** is formed, the following rearrangement reaction take place by a five- or six-membered cyclic transition state to yield compound **2** with more thermodynamically stable C–N bond than C–S bond. In addition, the rearrangement reaction for Hcy is much slower than Cys due to the less favourable six-membered cyclic transition state

than the five-membered one. On the other hand, in the case of GSH, after the thiol-halogen S_NAr nucleophilic substitution, the intramolecular rearrangement is difficult to happen due to the unstable macrocyclic transition state, thus it result in the stable product **3**.

Next, we evaluated the selectivity of **BODIPY-PPh₃** toward other amino acids. As shown in Fig. 3, only GSH triggered significant fluorescence ratio changes of 16.99. Cys and Hcy showed certain fluorescence responses but their fluorescence ratio was smaller compared to GSH (0.69 and 2.02 for Cys and Hcy, respectively). Other amino acids did not promote noticeable fluorescence variations. We further check the detection of GSH in the presence of other amino acids and metal ions (Fig. S3). The existence of other interferent did not affect the detection of GSH. The results confirmed the high selectivity of probe **BODIPY-PPh₃** for GSH.

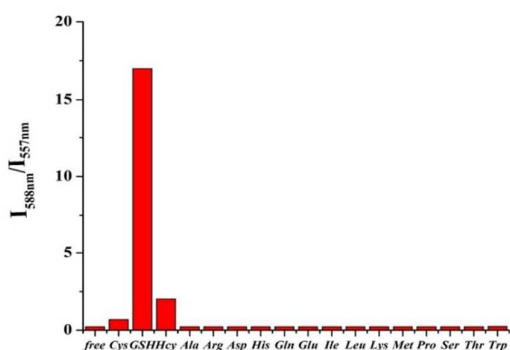


Fig. 3 Fluorescence intensity ratio (I_{588}/I_{557}) responses of **BODIPY-PPh₃** (10 μ M) upon addition of various amino acids (1mM) in acetonitrile/HEPES buffer (5:95 v/v, 20 mM, pH = 7.4) after 3 h addition at 37 °C. λ_{ex} = 550 nm.

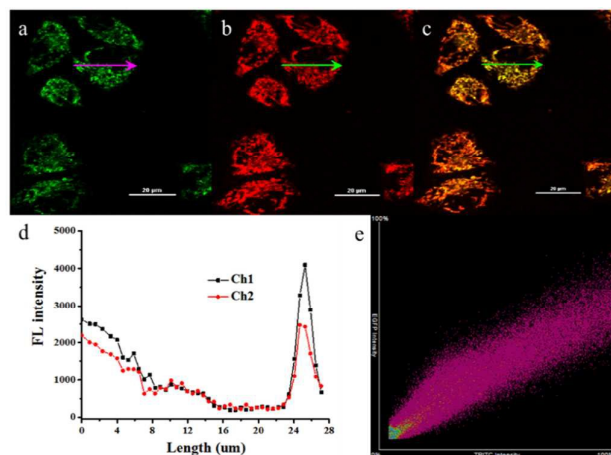


Fig. 4 Single cell colocalization of rhodamine 123 and **BODIPY-PPh₃** in mitochondria of HeLa cells. HeLa cells were pretreated with GSH (1mM) for 20min, and then costained with (a) rhodamine 123 (2 μ M, Channel 1 (Ch1), λ_{ex} 488 nm; λ_{em} 500–550 nm) and (b) **BODIPY-PPh₃** (2 μ M, Channel 2 (Ch2), λ_{ex} 561 nm; λ_{em} 570–620 nm). (c) Merged image of (a) and (b). (d) Intensity profile of region of interest 1 (ROI 1) cross the HeLa cell costained with Rh 123 and **BODIPY-PPh₃**. (e) Intensity scatter plot of Ch1 and Ch2.

To examine the mitochondrial-locating performance of **BODIPY-PPh₃**, colocalization experiments were conducted by costaining HeLa cells with a commercial mitochondrial tracker rhodamine 123 and **BODIPY-PPh₃**. The fluorescence of rhodamine 123 (Fig. 4a) from the costained cells in the presence of GSH overlaps well with that of **BODIPY-PPh₃** (Fig. 4b), as shown in the merged yellow image (Fig. 4c). Obviously, the changes in the intensity profiles of the linear region of interest (ROI) 1 across the living HeLa cell are synchronous in the two channels (Fig. 4d). More importantly, a high Pearson's coefficient of 0.96 and an overlap coefficient of 0.95 are obtained from the intensity correlation plots (Fig. 4e).

Meanwhile, in order to further approve the location of **BODIPY-PPh₃** in mitochondria, we studied the colocalization between the probe **BODIPY-PPh₃** and rhodamine 123 in multiple cell levels. Fig. S4 show that **BODIPY-PPh₃** and rhodamine 123 can colocalize in a plurality of living cells in the mitochondria, and high Pearson's colocalization coefficient 0.95 and overlap coefficient 0.95 indicate that the staining of **BODIPY-PPh₃** fits well with that of mitochondrial tracker rhodamine 123. The intensity profile of ROI 1 across HeLa cells in the two channels also varies in close synchrony. Besides, a high correlation is found in the intensity scatter plot of green and red channels, suggesting **BODIPY-PPh₃** exists predominantly for multiple cells in mitochondria. The results further confirmed that the probe can accurately locate and in the mitochondria of the cell.

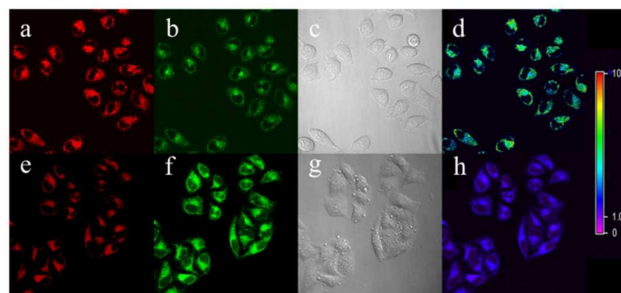


Fig. 5 Confocal fluorescence images of living HeLa cells incubated with GSH (1 mM) for 20 min, and then incubated with **BODIPY-PPh₃** (2 μ M) for 15 min: (a) red channel (λ_{ex} 561 nm; λ_{em} 570–620 nm); (b) green channel (λ_{ex} 488 nm; λ_{em} 500–550 nm); (c) bright-field transmission image; (d) ratio image generated from (a) and (b). Confocal fluorescence images of living HeLa cells incubated with NEM (1 mM) for 20 min, and then incubated with the **BODIPY-PPh₃** (2 μ M) for 15 min: (e) red channel (λ_{ex} 561 nm; λ_{em} 570–620 nm); (f) green channel (λ_{ex} 488 nm; λ_{em} 500–550 nm); (g) bright-field transmission image; (h) ratio image generated from (e) and (f).

The selective detections of GSH in the mitochondria of the living HeLa cells were carried out by using confocal fluorescence imaging. As shown in Fig. 5, when incubation with GSH for 20 min at 37 °C, and then incubation with **BODIPY-PPh₃** for 15 min, fluorescence from both green (500–550 nm) and red channels (570–620 nm) was observed (Fig. 5a and 5b). The fluorescence ratio of red/green channels was \sim 5 (Fig. 5d). By contrast, the incubation of *n*-ethylmaleimide (NEM) to trap intracellular thiols prior to the addition of **BODIPY-PPh₃** resulted in relatively weak emission in red channel and strong

COMMUNICATION

Journal Name

emission in green channel (Fig. 5e and f), and the fluorescence ratio decreased to ~2. (Fig.5h). It indicated that **BODIPY-PPH₃** is capable of monitoring GSH in the mitochondria of living cells.

In conclusion, we have developed a mitochondrial-targeting fluorescent probe **BODIPY-PPH₃** for the selective detection of GSH. The probe contained a triphenylphosphine as a mitochondrial targeting group and showed ratiometric response and selectivity for GSH over Cys/Hcy with high sensitivity. Colocalization experiments demonstrated that the probe specially located mitochondrial in living cells. Confocal fluorescence microscopy experiments confirmed its applicability to detect GSH in mitochondria of the living cells. We anticipate the probe can be used for exploring biological effects of mitochondrial GSH.

We thank Prof. Z. Niu (TIPC) for providing HeLa cells. This work was financially supported by the 973 program (2013CB933800), National Natural Science Foundation of China (21525206, 21402216, 21272243 and 61475164), the Fundamental Research Funds for the Central Universities and Beijing Municipal Commission of Education.

Notes and references

1. K.Henze and W. Martin, *Nature*, 2003, **426**, 127-128.
2. (a) T.Finkel, M.Serrano and M. A.Blasco, *Nature*, 2007, **448**, 767-774; (b) H.M. McBride, M. Neuspiel and S. Wasiak, *Curr. Biol.*, 2006, **16**, 551-660; (c) A. T.Hoye, J. E.Davoren, P.Wipf, M. P.Fink and V. E.Kagan, *Accounts. Chem. Res.*, 2008, **41**, 87-97; (d) V.Gogvadze, S.Orrenius and B.Zhivotovsky, *Semin. Cancer Biol.*, 2009, **19**, 57-66.
3. Y. Y. Wang, S. M.Chen and H. Li, *Acta Pharma. Sinica.*, 2010, **31**, 160-164.
4. (a) A. M.Strohecker and E. White, *Cancer Discov.*, 2014, **4**, 766; (b) R.E. E. amsay, P. J.Hogg and P. J.Dilda, *Pharm. Res.*, 2011, **28**, 2731; (c) P.W.Szlosarek, S. Lee and P. J.Pollard, *Mol. Cell.*, 2014, **56**, 343.
5. (a) H. J.Forman, H.Zhang and A.Rinna, *Mol. Aspects. Med.*, 2009, **30**, 1-12; (b) R.A.Smith, R.C.Hartly and M.P.Murphy, *Antioxid. Redox. Signal.*, 2011, **15**:3021-3038.
6. (a) M. Vendrell, D. Zhai, J. C. Er and Y.T. Chang, *Chem. Rev.*, 2012, **112**, 4391-4420; (b) H. Kobayashi, M. Ogawa, R. Alford, P. L. Choyke and Y. Urano, *Chem. Rev.*, 2010, **110**, 2620-2640; (c) R. W.Sinkeldam, N. J. Greco and Y. Tor, *Chem. Rev.*, 2010, **110**, 2579-2619;(d) Y. M. Yang, Q. Zhao, W.Feng, F. Y.Li, *Chem. Rev.*, 2013, **113**, 192-270. (e) H. Chen, Y. Tang and W. Lin, *TRAC-Trend. Anal. Chem.*, 2016, **76**, 166-181.
7. (a) X.-L. Liu, L.-Y. Niu, Y.-Z. Chen, Y. Yang and Q.-Z. Yang, *Biosens. Bioelectron.* 2016, doi: 10.1016/j.bios.2016.06.076; (b) L.-Y. Niu, Y.-S. Guan, Y.-Z. Chen, L.-Z. Wu, C.-H.Tung and Q.-Z.Yang, *J. Am. Chem. Soc.*, 2012, **134**, 18928-18931; (c) L.-Y. Niu, Y.-Z. Chen, H.-R. Zheng, L.-Z. Wu, C.-H. Tung and Q.-Z.Yang, *Chem. Soc. Rev.*, 2015, **44**, 6143-6160; (d) L.-Y. Niu, Q.-Q. Yang, H.-R. Zheng, Y.-Z. Chen, L.-Z. Wu, C.-H. Tung and Q.-Z. Yang, *RSC Adv.*, 2015, **5**, 3959-3964; (e) M.-Y. Jia, L.-Y. Niu, Y. Zhang, Q.-Z. Yang, C.-H. Tung, Y.-F. Guan and L. Feng, *ACS Appl. Mater. Interfaces.*, 2015, **7**, 5907-5914; (f) H. Li, J. Fan, J. Wang, M. Tian, J. Du, S. Sun, P. Sun and X. Peng, *Chem. Commun.*, 2009, **39**, 5904-5906; (g) X. Wang, J. Lv, X. Yao, Y. Li, F. Huang, M. Li, J. Yang, X. Ruan and B. Tang, *Chem. Commun.*, 2014, **50**, 15439-15442; (h) F. Y. Wang, L. Zhou, C. C. Zhao, R. Wang, Q. Fei, S. H. Luo, Z. Q. Guo, H. Tian and W. H. Zhu, *Chem. Sci.*, 2015, **6**, 2584-2589; (i) X. Yang, Y. Guo and R. M. Strongin, *Angew. Chem. Int. Ed.*, 2011, **50**, 10690-10693; (j) J. Zhang, J. Wang, J. Liu, L. Ning, X. Zhu, B. Yu, X. Liu, X. Yao and H. Zhang, *Anal. Chem.*, 2015, **87**, 4856-4863. (k) H. Chen, Y. Tang, M. Ren and W. Lin, *Chem. Sci.*, 2016, **7**, 896-1903; (l) J. Y. Wang, Z.-R. Liu, M. Ren, X. Kong and W. Lin, *J. Mater. Chem. B*, 2017, DOI: 10.1039/C6TB02610A; (l) L. He, Q. Xu, Y. Liu, H. Wei, Y. Tang and W. Lin, *ACS Appl. Mater. Interfaces*, 2015, **7**, 12809-12813
8. (a) H. Zhang, C. X. Wang, K. Wang, X.P. Xuan, Q. Z. Lv and K. Jiang, *Biosens. Bioelectron.*, 2016, **85**, 96-102; (b) J. Zhang, X. L. Bao, J. L. Zhou, F. F. Peng, H. Ren, X. C. Dong and W. L. Zhao, *Biosens. Bioelectron.*, 2016, **85**, 164-170; (c) S. Y. Lim, K. H. Hong, D. R. Kim, H. Kwon and H. J. Kim, *J. Am. Chem. Soc.*, 2014, **136**, 7018-7025; (d) X. Zheng and X. Lin, *Chem. Commun.*, 2015, **52**, 1094-1119.
9. L.-Y. Niu, Y.-Shi. Guan, Y.-Z. Chen, L.-Z. Wu, C.-H. Tunga and Q.-Z. Yang, *Chem. Commun.*, 2013, **49**, 1294-1296.
10. (a) S.I. Nigam, B. P. Burke and L. H. Davies, *Chem. Commun.*, 2016, **52**, 7114-7117; (b) H. B. Yu, X. F. Zhang, Y. Xiao, W.Zou, L.P. Wang and L. J. Jin, *Anal. Chem.*, 2013, **85**, 7076-7084; (c) J. Zhou, L. H. Li, W. Shi, X. H. Gao, X. H. Li and H. M. Ma, *Chem. Sci.*, 2015, **6**, 4884-4888; (d) J. Xu, Y. Zhang, H. Yu, X. D.Gao and S. J.Shao, *Anal. Chem.*, 2016, **88**, 1455-1461; (e) P. Ning, J.C. Jiang, L. C. Li, S. X. Wang, H. Z. Yu, Y. Feng, M. Z. Zhu, B. C. Zhang, H. Yin, Q. X. Guo and X. M. Meng, *Biosens. Bioelectron.*, 2016,**77**, 921-927; (f) X. Y. Gong, X. F.Yang, Y. Y. Zhong, Y. H. Chen and Z. Li, *Dyes and Pigments.*, 2016, **131**, 24-32; (g) B.N. Sui, S. Tang, A. W. Woodward, B. Kim and K. D. Belfield, *Eur. J. Org. Chem.*, 2016, 2851-2857.
11. M. P. Murphy and R. A. J. Smith, *Annu. Rev. Pharmacol. Toxicol.*, 2007, **47**, 629-656.